

## Article

# Modern Dimensional Analysis Based on Fire-Protected Steel Members' Analysis Using Multiple Experiments

Pál-Botond Gálfi<sup>1</sup>, Renáta-Ildikó Száva<sup>1</sup> , Ioan Száva<sup>1,\*</sup> , Sorin Vlase<sup>1,2,\*</sup> , Teofil Gălăţanu<sup>1</sup>,  
Károly Jármái<sup>3</sup> , Zsolt Asztalos<sup>1</sup> and Gabriel Popa<sup>1</sup>

<sup>1</sup> Department of Mechanical Engineering, Transilvania University of Brasov, B-dul Eroilor 29, 500036 Brasov, Romania

<sup>2</sup> Romanian Academy of Technical Sciences, 100562 Bucharest, Romania

<sup>3</sup> Faculty of Mechanical Engineering, University of Miskolc, 3515 Miskolc, Hungary

\* Correspondence: eet@unitbv.ro (I.S.); svlase@unitbv.ro (S.V.)

**Abstract:** Nowadays, the real structures (considered as prototypes) subjected to fire are analysed by means of the behaviours of some reduced scale structures (defined as models). These prototype–model correlations are governed by the so-called dimensional analysis (DA) methods. These methods, starting from the Buckingham theorem, offer several dimensionless variables and based on them is the so-called Model Law (*ML*), which is able to foresee the predictable prototype's answer based on the results of the experimental investigations performed exclusively on the model (usually manufactured at a reduced scale). Based on the MDA principles, in a previous paper the authors elaborated the complete *ML* for the heat transfer in beams with rectangular-hole cross-sections, considering unprotected as well as thermally protected structural elements. The authors, based on meticulous experimental investigations, obtained the validation of this *ML* for the unprotected steel members. In this contribution, the authors offer in a similar manner the *ML* validation for intumescent paint-protected steel members and thus the complete validation of their original *ML*. In their theoretical and experimental investigations, the authors involved both a real column's element combined with its models manufactured at 1:2 and 1:4, as well as 1:10 scales too. Consequently, the obtained *ML* can be considered as generally valid, involving a real structural element and its model manufactured at the desired scale.

**Keywords:** Modern Dimensional Analysis; Model Law; steel column; heat transfer; intumescent paint; multiple experiments



**Citation:** Gálfi, P.-B.; Száva, R.-I.; Száva, I.; Vlase, S.; Gălăţanu, T.; Jármái, K.; Asztalos, Z.; Popa, G. Modern Dimensional Analysis Based on Fire-Protected Steel Members' Analysis Using Multiple Experiments. *Fire* **2022**, *5*, 210. <https://doi.org/10.3390/fire5060210>

Academic Editor: Tiago Miguel Ferreira

Received: 8 November 2022

Accepted: 5 December 2022

Published: 8 December 2022

**Publisher's Note:** MDPI stays neutral with regard to jurisdictional claims in published maps and institutional affiliations.



**Copyright:** © 2022 by the authors. Licensee MDPI, Basel, Switzerland. This article is an open access article distributed under the terms and conditions of the Creative Commons Attribution (CC BY) license (<https://creativecommons.org/licenses/by/4.0/>).

## 1. Introduction

It is a well-known fact that during a fire all structural elements will reduce their mechanical properties, which has to be prevented using different heat insulation solutions [1–7]. Between these solutions, one can mention intumescent paint which preserves the initial structural elements' suppleness together with its strength. The fire resistance problem is analysed deeply in several references, such as [8–11], respectively [12–17]. One other significant issue is the fire modelling [18,19], as well as the introduced thermal flow accurate evaluation [20–22]. During the last century, based on the model–prototype correlations, new approaches were conceived and introduced such as Geometric Analogy (GA) and Theory of Similarity (*TS*), as well as Classical Dimensional Analysis (CDA) (mainly for the complex processes) [23–34].

Their applicability is strongly limited due to several shortcomings [35–45], analysed in detail by the authors in [1,46–58]. Even CDA represents a relatively general approach; it also has several limits, including representing a relatively chaotic procedure in the identification of the dimensionless variables  $\pi_j, j = 1, \dots, n$ , necessary in establishing the desired Model Law (*ML*). One other difficulty involves requiring solid theoretical knowledge in both of the

analysed phenomena, but also in higher mathematics too, which limit its wide application in common engineering problems. CDA only allows, in very limited and particular cases, the obtaining of the complete *ML* and it represents a relatively unyielding method, without allowing the obtaining of a flexible prototype–model correlation.

On the contrary, its new version, developed by Szirtes in [59,60] and referred to hereinafter as Modern Dimensional Analysis (MDA), offers a very flexible and efficient approach which is easy to apply by any common researcher. In their previous contributions, the advantages of MDA in different engineering areas were analysed and illustrated [1,55–58,61]. One of their major fields of applicability was the heat transfer problem in massive-as well as tubular cross-sectional steel structural elements [55–58,61–64].

These last-mentioned contributions also offer a critical and comparative analysis of the aforementioned methods with respect to MDA. Among the main advantages of MDA one has to mention its unitary approach and its simplicity, as well as its potential for offering the complete set of *ML*, which practically is not offered by any of the aforementioned approaches. From this complete set of *ML*, one can obtain, without any difficulties, different particular cases of the analysed phenomenon and so can assign the most suitable model to the analysed prototype.

## 2. Materials and Methods

As mentioned before in [64], the authors, based on the deduced *ML* in [57], performed a searching experimental investigation in order to validate the obtained *ML* for the case of the unprotected (without an intumescent paint layer) steel members.

In the following work, these results will be briefly summarised in order to assure a continuity of the analysed phenomenon with the actual-presented research results of the authors.

They conceived, manufactured and tested an original electric testing bench, described in [1,56,64]. The main components of this testing bench are shown in Figure 1. Figure 2 and Table 1 offer the main dimensions (sizes) of the tested structural elements.

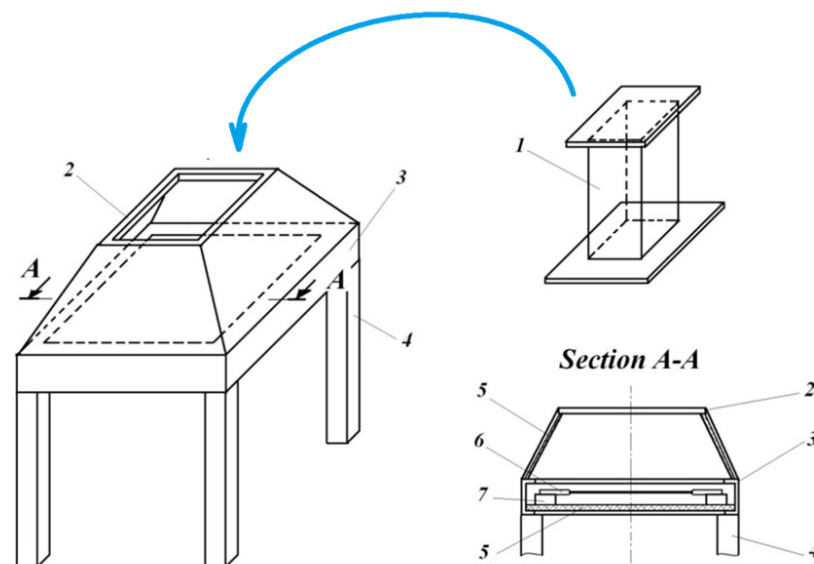


**Figure 1.** The original testing bench [1,56,64]: 1-tested structural element; 2-dome in form of pyramid trunk; 3-rigid frame; 4-supporting legs; 5-heat insulation layer; 6-heating elements (Silite rods); 7-chamotte bricks. The blue arrow shows how the tested element has to be placed on/over the dome 2.

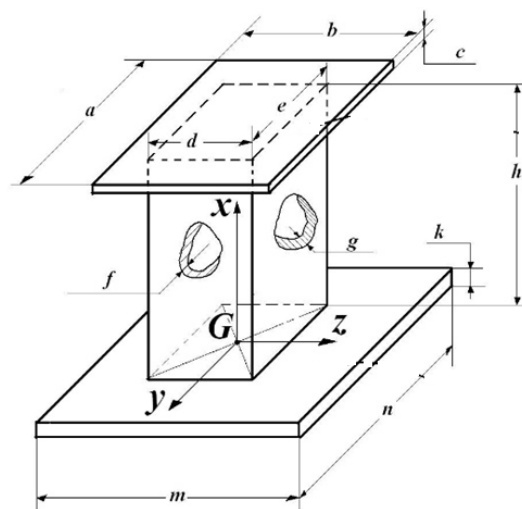


Figure 2. The tested structural elements' sizes [1,56,64].

Table 1. The structural elements' sizes [1,56,64].

| Dimensions,<br>in <i>m</i> | The Scale of the Tested Element |       |        |        |
|----------------------------|---------------------------------|-------|--------|--------|
|                            | 1:1                             | 1:2   | 1:4    | 1:10   |
| <i>a</i>                   | 0.370                           | 0.185 | 0.108  | 0.0370 |
| <i>b</i>                   | 0.370                           | 0.185 | 0.108  | 0.0370 |
| <i>c</i>                   | 0.006                           | 0.003 | 0.0015 | 0.0015 |
| <i>d</i>                   | 0.350                           | 0.175 | 0.0875 | 0.0030 |
| <i>e</i>                   | 0.350                           | 0.175 | 0.0875 | 0.0030 |
| <i>f</i>                   | 0.016                           | 0.008 | 0.004  | 0.0015 |
| <i>g</i>                   | 0.016                           | 0.008 | 0.004  | 0.0015 |
| <i>h</i>                   | 0.400                           | 0.200 | 0.100  | 0.400  |
| <i>k</i>                   | 0.010                           | 0.005 | 0.0025 | 0.0015 |
| <i>m</i>                   | 0.450                           | 0.450 | 0.450  | 0.450  |
| <i>n</i>                   | 0.450                           | 0.450 | 0.450  | 0.450  |

In their investigations, the authors started from a real pillar manufactured at scales 1:1; 1:2; 1:4, respectively, and 1:10 for the prototype as well as related models. Consequently, they obtained 6 sets of prototypes and models, i.e., (1:1–1:2); (1:1–1:4); (1:1–1:10); (1:2–1:4); (1:2–1:10); and (1:4–1:10), which were initially unprotected with intumescent paint. They applied the same heating conditions to all of them and monitored all of the involved parameters. How they will be analysed is explained in the following: if a structural element plays the role of the prototype, than practically all of its variables are considered to be independent (they are chosen a priori both for the prototype and for the model). However, some are to be determined by the *ML*; these variables are considered to be dependent ones. Consequently, during the investigations, a part of the data will be considered as data directly acquired by measurements and others as reference elements for those, which will be obtained with the *ML* obtained by applying MDA. The quantities of direct measurements (on the elements, which were considered as models) were compared with those obtained with *ML* (corresponding to the elements taken as prototypes), resulting in a very good correlation; these prove the *ML* validity for different/desired scales of the models.

In order to evaluate the thermal insulation performance of the testing bench, one can mention that at a nominal heating temperature  $t_{o,nom} = 600$  °C of the tested structural elements, the maximal temperature around the testing bench was less than (45–50) °C.

The efficiency of the original electronic control and regulation system [62] can also be evaluated by means of a very quick self-learning behaviour, i.e., after a maximum of two cycles passing over a  $t_{o,nom} = (500\text{--}600) \text{ }^\circ\text{C}$  nominal temperature value, with the thermal/temperature oscillation not exceeded  $(5\text{--}8) \text{ }^\circ\text{C}$ .

Additionally, for a  $t_{o,nom} = (500\text{--}600) \text{ }^\circ\text{C}$  nominal temperature the electric consumption is approx. 25 kW, allowing a general-purpose application of this testing bench, as well as its use in very modestly equipped laboratories too.

Due to the rigorously identical thermal regimes of all tested elements, i.e., in reaching the same temperatures  $t_{o,nom}(\text{ }^\circ\text{C})$ , the scale factor of the temperatures was the same  $S_{\Delta t} = \frac{\Delta t_2}{\Delta t_1} = ct = 1$ , no longer appearing in the *ML* and resulting in a simplified expression of them.

The main steps of the experimental investigations were the following:

- the stand mounting, with the adequate thermal insulation;
- the mounting of the tested structural element on the lower plate (*mxn*);
- checking the functioning of the test bench;
- the checking of the nominal temperature  $t_{o,nom}$ ;
- the checking of the heating regime's steps;
- starting the test bench and monitoring all heating parameters, such as:
  - the consumed electrical energy  $E_{o,total}$  [kWh] the time  $\tau_{o,total}$  [s] corresponding to the stabilised thermal regime, which was considered when the maximal temperature oscillation of  $(0.2\text{--}0.3) \text{ }^\circ\text{C}$  was observed for a minimum period of  $(120\text{--}180)$ s at the upper part of the tested structural element;
  - the repeating of these stages for all nominal values of  $t_{o,nom} = (100, 200, 300, 400, 450, 500) \text{ }^\circ\text{C}$ .

Corresponding to a stabilised regime, the heat amount was considered such as:

$$Q_{o,total}[\text{J}] = E_{o,total} \times 3.6 \times 10^6. \tag{1}$$

because

$$1 \text{ kWh} = 3600 \text{ kW} \cdot \text{s} = 3600 \text{ kJ} = 3.6 \times 10^6 \text{ J}$$

The total heat losses over the thermal insulation layers are offered by:

$$Q_{waste,total} = Q_{w,total} = \sum [\lambda \cdot \Delta t \cdot \Delta \tau \cdot (\sum \frac{A_k}{h_k})]. \tag{2}$$

where  $\lambda(\frac{\text{W}}{\text{m}\cdot\text{K}} = \frac{\text{W}}{\text{m}\cdot\text{ }^\circ\text{C}})$  is the thermal insulation layer's thermal conductivity coefficient, offered by the manufacturer, depending on the heated site's temperature  $t[\text{ }^\circ\text{C}]$ :

$$\lambda(\frac{\text{W}}{\text{m}\cdot\text{ }^\circ\text{C}}) = 0.0002 \times t(\text{ }^\circ\text{C}) + 0.03, \tag{3}$$

$\Delta t(\text{ }^\circ\text{C})$ —temperature difference reached during heating;

$\Delta \tau(\text{ s})$ —the corresponding time;

$A_k(\text{ m}^2)$ —the unfolded areas of the  $k$  heat-insulating layer applied around the testing bench, with the thickness  $h_k(\text{ m})$ .

Due to the particularity of the heating system's thermo-regulation, which acts in well-defined steps instead of a linear law from  $t_B \equiv t_i$  to  $t_D \equiv t_n$  (the broken line in Figure 3), i.e., a funicular polygon ( $B \equiv i - j - k - l - m - n \equiv D$ ), the Equations (1) and (2) will be adapted as follows:

- In Equation (1) for each interval  $(i - j); (j - k); (k - l); (l - m); (m - n)$ , the corresponding temperature difference [ $\Delta t_{ij} = (t_j - t_i); \Delta t_{jk} = (t_k - t_j); \Delta t_{kl} = (t_l - t_k); \Delta t_{mn} = (t_n - t_m)$ ] will be considered and applied to the  $\Delta \tau$  time intervals corresponding to  $\Delta \tau_{ij} = (\tau_j - \tau_i); \Delta \tau_{jk} = (\tau_k - \tau_j); \Delta \tau_{kl} = (\tau_l - \tau_k); \Delta \tau_{lm} = (\tau_m - \tau_l); \Delta \tau_{mn} = (\tau_n - \tau_m)$ ;

- With Equation (2),  $\lambda$  will be determined individually for each interval prior, considering the average temperature related to each interval and the temperature differences prior, respectively;
- The term  $\sum \frac{A_k}{h_k}$  will be constant; it will multiply the sum of the partial products related to these intervals.

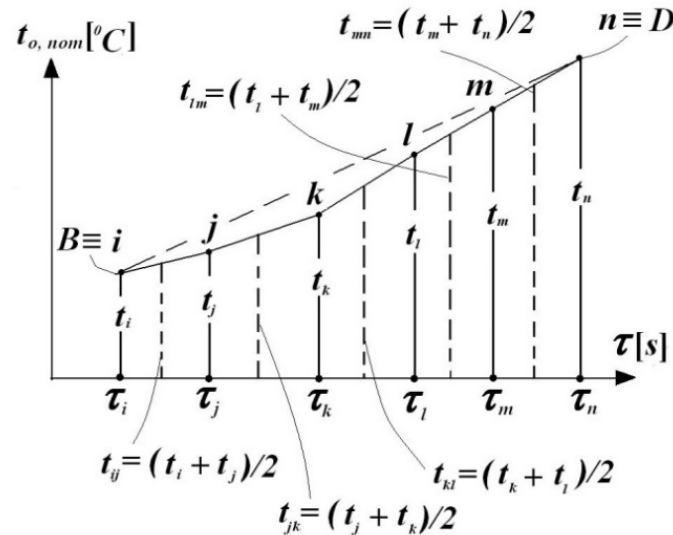


Figure 3. The particularity of the heating system’s thermo-regulation [56,64].

The invested heat  $Q_{total}$  (J) will be the difference of the previous ones, i.e.,

$$Q_{total}[J] = Q_{0,total} - Q_{w,total} \tag{4}$$

Additionally, taking into consideration that only 47.22% of the Silite bars’ radiation will arrive directly to the lower part of the tested structural elements, and will correspond to the angle  $(2 \times 85^\circ)$  from the total of  $360^\circ$  (Figure 4), one can define the effective invested heat in the system, i.e.,

$$Q_{eff}[J] = Q_{o,eff} - Q_{w,total} = 0.4722 \cdot Q_{o,total} - Q_{w,total} \tag{5}$$

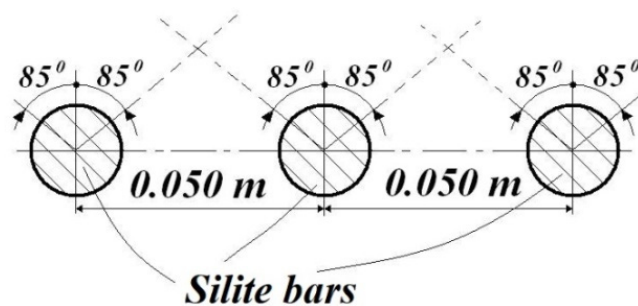


Figure 4. The effective heat transfer offered by the Silite bars [56,64].

One has to mention that the  $ML$  was also validated for the case of Equation (5). Based on the definition of the heat flux  $\dot{Q}$ , one has:

$$\dot{Q} \left( \frac{J}{s} = W \right) = \frac{dQ}{d\tau} = \frac{\Delta Q}{\Delta \tau} \tag{6}$$

All of the above-mentioned and defined variables will be obtained by summing the last values with those previously obtained, e.g., the parameters related to the stabilised

regime at  $t_{0,nom} = 200$  °C result from summing the corresponding values of  $t_{0,nom} = 100$  °C with those obtained during the heating of the system in the temperature range (100–200)°C.

Taking into consideration the aforementioned *ML*, synthesised in [57] and applied in [64] for the unprotected steel structural elements, in this contribution the authors performed its validation for the intumescent-paint-protected steel members.

In this sense, one has to summarise some facilities of the MDA:

MDA allows a priori choosing for both prototype and model of the set of variables (the independent ones), which are directly related to the experimental measurements (performed only on the model!);

The rest of the variables (the dependent ones) are chosen freely a priori only for the prototype; in the case of the model, these variables' magnitude are obtained exclusively with the elements of *ML*, based on scrupulous experiments performed on the model;

Only a few numbers of variables for the prototype are excepted, that is those ones which cannot be easily determined by measurements; these are obtained using the *ML*, of course based on rigorous measurements performed on the model;

MDA, based on a suitable choice of independent variable, allows the waiving of the restrictions of Geometric Analogy (so that the model is geometrically similar to the prototype); for example, the cross-section of the model may be different in shape from the prototype, etc., as well as with regards to choosing different materials for the prototype and the model.

Several other facilities of MDA are synthesised both in Szirtes' references [59,60], as well as in the previous ones of the authors [1,55–58,64].

As was mentioned before, the complete set of the *ML*, where two versions have practical significance, was obtained in [57], i.e.,

Version I, with  $(Q, L_z, \Delta t, \tau, \lambda_{x\ steel}, \zeta)$  as the set of independent variables, where the following dependent variables were selected from the obtained *ML*:

$$S_{\dot{Q}} = \frac{S_Q}{S_\tau}, \quad (7)$$

$$S_{A_{tr}} = \frac{S_{L_z}}{S_\zeta}. \quad (8)$$

Version II, with  $(\dot{Q}, L_z, \Delta t, \tau, \lambda_{x\ steel}, \zeta)$  as the set of independent variables, from where the following were chosen:

$$S_Q = S_{\dot{Q}} \cdot S_\tau, \quad (9)$$

$$S_{A_{tr}} = \frac{S_{L_z}}{S_\zeta}, \quad (10)$$

where  $Q$ (J) is the invested heat;  $\dot{Q}$ (W)—the heat rate;  $L_z$ (m)—the beam dimension along direction  $z$ ;  $\Delta t$ (°C)—the temperature variation;  $\tau$ (s)—the time;  $\lambda_{x\ steel}$ ( $\frac{W}{^\circ C \cdot m}$ )—the thermal conductivity;  $\zeta = \frac{P}{A}(\frac{1}{m})$ —the shape factor;  $P$ (m)—the perimeter of the cross-section;  $A$ (m<sup>2</sup>)—the area of the cross-section; and  $S_\omega = \frac{\omega_2}{\omega_1}(-)$ —the scale factor of the variable  $\omega$ , with index "1" for the prototype and "2" for the model, respectively.

Useful remarks:

- The quadratic section represents a particular case of the rectangular one, with the same dimensions and the same scale factors along the  $z$  and  $y$  cross-sectional coordinates;
- The MDA allows the defining of different thicknesses ( $\delta_z \neq \delta_y$ ) as well as different sizes ( $L_z \neq L_y$ ) along the  $z$  and  $y$  cross-sectional directions, which subsequently will be defined by the corresponding elements of the *ML*;
- When the length  $L_z$  is considered an independent variable, i.e., freely chosen a priori for both prototype and model, the corresponding elements of *ML* ( $L_x, L_y, \delta_y\ steel, \delta_z\ steel$ ) can be ignored; one is accepted as having the same scale factor of length  $S_L$ ;

- By selecting the shape factor  $\zeta$  as an independent variable, together with the length  $L_z$ , MDA offers a great opportunity for the model to be freed from the geometric similarity restriction of the cross-sections for the prototype and the model (e.g., one can accept different cross-sections, not only rectangular ones, with the single condition having the foreseen shape factor  $\zeta$ );
- One has to mention that, in both cases, the independent variables are rigorously related to the actual measurements;
- Only one dependent variable represents an exception, that is the one for which one has considered having limited access to the prototype (or which will be difficult to measure) and where one has to be obtained by means of the ML. In the case of Version I, this dependent variable was considered the heat flow  $\dot{Q}$ , while in the case of Version II, this is the amount of heat  $Q$ .

### 3. Results

As was mentioned in Sections 2 and 3, all tested structural elements protected with intumescent paint layers (even when they were considered as a prototype or model), were monitored for significant data, such as the total consumed electrical energy  $E_{o,total}$  [kWh], the corresponding total invested heat amount  $Q_{o,total}$  [J] applying Equation (1) and the total heat losses over the thermal insulation layers  $Q_{w,total}$  [J] using Equation (2), as well as the corresponding total heat  $Q_{total}$  [J] as a difference between  $Q_{o,total}$  [J] and  $Q_{w,total}$  [J], by applying Equation (4), synthesised in Table 2.

Table 2. Preliminary data.

| Tested Structural Element, All Painted | $\Delta t$ [°C] | $\zeta[\frac{1}{m_y}]$ | $E_{0,total}$ kWh | $Q_{o,total}$ [J] | $\Delta t_{total}$ [°C] | $\sum \frac{A_k}{h_k}$ [m] | $Q_{w,total}$ [J] | $Q_{total}$ [J] |
|--|-----------------|------------------------|-------------------|-------------------|-------------------------|----------------------------|-------------------|-----------------|
| at scale 1:10                          | 23–100          | 0.7017543              | 0.4               | 1,440,000         | 77                      | 20.34095                   | 16,958.25002      | 1,423,041.75    |
|  | 100–200         | 0.7017543              | 0.7               | 2,520,000         | 100                     | 20.34095                   | 37,242.24536      | 2,482,757.755   |
|  | 200–300         | 0.7017543              | 0.6               | 2,160,000         | 100                     | 20.34095                   | 15,238.33319      | 2,144,761.667   |
|  | 300–400         | 0.7017543              | 0.8               | 2,880,000         | 100                     | 20.34095                   | 32,726.55446      | 2,847,273.446   |
|  | 400–450         | 0.7017543              | 0.5               | 1,800,000         | 50                      | 20.34095                   | 22,656.56375      | 1,777,343.436   |
|  | 450–500         | 0.7017543              | 0.5               | 1,800,000         | 50                      | 20.34095                   | 12,894.12821      | 1,787,105.872   |
| at scale 1:4                           | 23–100          | 0.2619760              | 0.4               | 1,440,000         | 77                      | 20.07323                   | 73,312.41894      | 1,366,687.581   |
|  | 100–200         | 0.2619760              | 1.0               | 3,600,000         | 100                     | 20.07323                   | 411,563.842       | 3,188,436.158   |
|  | 200–300         | 0.2619760              | 1.6               | 5,760,000         | 100                     | 20.07323                   | 1,016,681.839     | 4,743,318.161   |
|  | 300–400         | 0.2619760              | 1.0               | 3,600,000         | 100                     | 20.07323                   | 685,259.6097      | 2,914,740.39    |
|  | 400–450         | 0.2619760              | 0.9               | 3,240,000         | 50                      | 20.07323                   | 706,478.8158      | 2,533,521.184   |
|  | 450–500         | 0.2619760              | 2.3               | 8,280,000         | 50                      | 20.07323                   | 2,287,112.765     | 5,992,887.235   |
| at scale 1:2                           | 23–100          | 0.1309880              | 0.6               | 2,160,000         | 77                      | 19.17165                   | 35,855.38923      | 2,124,144.611   |
|  | 100–200         | 0.1309880              | 1.3               | 4,680,000         | 100                     | 19.17165                   | 329,675.8286      | 4,350,324.171   |
|  | 200–300         | 0.1309880              | 1.0               | 3,600,000         | 100                     | 19.17165                   | 277,713.1232      | 3,322,286.877   |
|  | 300–400         | 0.1309880              | 1.6               | 5,760,000         | 100                     | 19.17165                   | 823,809.1535      | 4,936,190.847   |
|  | 400–450         | 0.1309880              | 0.7               | 2,520,000         | 50                      | 19.17165                   | 368,480.895       | 2,151,519.105   |
|  | 450–500         | 0.1309880              | 0.8               | 2,880,000         | 50                      | 19.17165                   | 544,542.1814      | 2,335,457.819   |
| at scale 1:1                           | 23–100          | 0.0654940              | 1.3               | 4,680,000         | 77                      | 15.55354                   | 34,080.0952       | 4,645,919.905   |
|  | 100–200         | 0.0654940              | 2.9               | 10,440,000        | 100                     | 15.55354                   | 426,290.5755      | 10,013,709.42   |
|  | 200–300         | 0.0654940              | 2.2               | 7,920,000         | 100                     | 15.55354                   | 343,502.9552      | 7,576,497.045   |
|  | 300–400         | 0.0654940              | 2.0               | 7,200,000         | 100                     | 15.55354                   | 330,213.3152      | 6,869,786.685   |
|  | 400–450         | 0.0654940              | 1.2               | 4,320,000         | 50                      | 15.55354                   | 242,363.0521      | 4,077,636.948   |
|  | 450–500         | 0.0654940              | 1.4               | 5,040,000         | 50                      | 15.55354                   | 515,674.9588      | 4,524,325.041   |

In a similar manner, this data evaluation was continued in Table 3, seen in the directly invested heat amount  $Q_{o,eff} = 0.4722 \cdot Q_{o,total}$  and the corresponding effective invested heat  $Q_{eff}$  [J] by means of Equation (5), as well as the corresponding heat fluxes by applying Equation (6) for its particular forms.

**Table 3.** Preliminary data.

| Tested Structural Element, All Painted | $\Delta t [^{\circ}\text{C}]$ | $Q_{o,eff}[\text{J}]$ | $Q_{eff}[\text{J}]$ | $\Delta\tau_{total}[\text{s}]$ | $\dot{Q}_{w,total}[\text{J}]$ | $\dot{Q}_{total}[\text{W}]$ | $\dot{Q}_{eff}[\text{W}]$ |
|--|-------------------------------|-----------------------|---------------------|--------------------------------|-------------------------------|-----------------------------|---------------------------|
| at scale 1:10                          | 23–100                        | 679,968               | 663,009.75          | 2070                           | 8.192391312                   | 687.4597826                 | 320.2945652               |
|  | 100–200                       | 1,189,944             | 1,152,701.755       | 2670                           | 13.9484065                    | 929.8718182                 | 431.7235036               |
|  | 200–300                       | 1,019,952             | 1,004,713.667       | 1020                           | 14.93954235                   | 2102.707516                 | 985.0133988               |
|  | 300–400                       | 1,359,936             | 1,327,209.446       | 1626                           | 20.12703226                   | 1751.09068                  | 816.2419714               |
|  | 400–450                       | 849,960               | 827,303.4363        | 960                            | 23.60058724                   | 1851.399413                 | 861.7744128               |
|  | 450–500                       | 849,960               | 837,065.8718        | 510                            | 25.28260432                   | 3504.12916                  | 1641.305631               |
| at scale 1:4                           | 23–100                        | 679,968               | 606,655.5811        | 2220                           | 33.02361213                   | 615.6250365                 | 273.2682798               |
|  | 100–200                       | 1,699,920             | 1,288,356.158       | 3720                           | 110.6354414                   | 857.1064941                 | 346.3323005               |
|  | 200–300                       | 2,719,872             | 1,703,190.161       | 3180                           | 319.7112702                   | 1491.609484                 | 535.5943901               |
|  | 300–400                       | 1,699,920             | 1,014,660.39        | 1320                           | 519.1360679                   | 2208.136659                 | 768.6821139               |
|  | 400–450                       | 1,529,928             | 823,449.1842        | 1020                           | 692.62629                     | 2483.844298                 | 807.3031218               |
|  | 450–500                       | 3,909,816             | 1,622,703.235       | 2700                           | 847.0788018                   | 2219.587865                 | 601.0011982               |
| at scale 1:2                           | 23–100                        | 1,019,952             | 984,096.6108        | 1260                           | 28.45665812                   | 1685.829056                 | 781.0290562               |
|  | 100–200                       | 2,209,896             | 1,880,220.171       | 2520                           | 130.8237415                   | 1726.319116                 | 746.1191156               |
|  | 200–300                       | 1,699,920             | 1,422,206.877       | 960                            | 289.2845034                   | 3460.715497                 | 1481.465497               |
|  | 300–400                       | 2,719,872             | 1,896,062.847       | 1560                           | 528.0827907                   | 3164.224902                 | 1215.424902               |
|  | 400–450                       | 1,189,944             | 821,463.105         | 540                            | 682.3720278                   | 3984.294639                 | 1521.227972               |
|  | 450–500                       | 1,359,936             | 815,393.8186        | 660                            | 825.0639111                   | 3538.572452                 | 1235.44518                |
| at scale 1:1                           | 23–100                        | 2,209,896             | 2,175,815.905       | 1680                           | 20.28577095                   | 2765.428515                 | 1295.128515               |
|  | 100–200                       | 4,929,768             | 4,503,477.425       | 3960                           | 107.6491352                   | 2528.714501                 | 1137.241774               |
|  | 200–300                       | 3,739,824             | 3,396,321.045       | 1560                           | 220.194202                    | 4856.728875                 | 2177.128875               |
|  | 300–400                       | 3,399,840             | 3,069,626.685       | 900                            | 366.9036836                   | 7633.096316                 | 3410.696316               |
|  | 400–450                       | 2,039,904             | 1,797,540.948       | 480                            | 504.9230253                   | 8495.076975                 | 3744.876975               |
|  | 450–500                       | 2,379,888             | 1,864,213.041       | 840                            | 613.8987605                   | 5386.10124                  | 2219.30124                |

For the ML validation in these two above-mentioned versions (I and II, respectively), the authors performed all calculi related to the significant. Considering Version I, with the independent variables ( $Q, L_z, \Delta t, \tau, \lambda_{x\ steel}, \zeta$ ), the main dependent variable was considered to be the heat flux  $\dot{Q}$ , determined by means of the ML for the prototype (based on the measurements made on the model).

In a similar manner, for the second version, with the independent variables ( $\dot{Q}, L_z, \Delta t, \tau, \lambda_{x\ steel}, \zeta$ ), the heat amount  $Q$  remains as the main dependent variable for the prototype.

In the described experimental investigations, all variables were determined using direct measuring/measurements. The real problem consisted of finding the aforementioned dependent variables through the ML for the analysed two versions in order to validate the ML.

In order to perform a rigorous analysis, the following prototype–model sets were considered:

- Prototype (structural element manufactured at 1:1 scale)—model (structural element at 1:2 scale), symbolised by (1:2/1:1) Model/Prototype;
- (1:4/1:2) Model/Prototype;
- (1:4/1:1) Model/Prototype;
- (1:2/1:10) Model/Prototype;
- (1:4/1:10) Model/Prototype;
- (1:4/1:10) Model/Prototype.

Based on the above-mentioned sets, each structural element has a well-defined role (either prototype or model). Consequently, a part of the measurement data was considered as data acquired directly through measurements, and others were taken as reference values for those that should be obtained through ML.

In Tables 4 and 5 the obtained results for Version I are summarised, respectively, and in Tables 6 and 7 there are those corresponding to Version II.

**Table 4.** Version I. Values obtained using direct measurements.

| Model/Prototype<br>(All Protected with<br>Intumescent Paint) | Measured Values                            |                 |                              |                     |                   |
|--|--|-----------------|------------------------------|---------------------|-------------------|
|  | Tmin-Tmax<br>$\Delta t [^{\circ}\text{C}]$ | $S_{\zeta} [-]$ | $S_{\Delta\tau_{total}} [-]$ | $S_{Q_{total}} [-]$ | $S_{Q_{eff}} [-]$ |
| 1:2/1.0  | 23–100                                     | 2               | 0.75                         | 0.457206464         | 0.452288545       |
|  | 100–200                                    | 2               | 0.636364                     | 0.434436829         | 0.417504074       |
|  | 200–300                                    | 2               | 0.615385                     | 0.438499066         | 0.418749246       |
|  | 300–400                                    | 2               | 1.733333                     | 0.718536262         | 0.617685159       |
|  | 400–450                                    | 2               | 1.125                        | 0.527638711         | 0.456992708       |
|  | 450–500                                    | 2               | 0.785714                     | 1.026875802         | 0.437393045       |
| 1:4/1:2  | 23–100                                     | 2               | 1.761905                     | 0.643406091         | 0.616459374       |
|  | 100–200                                    | 2               | 1.47619                      | 0.732919211         | 0.685215581       |
|  | 200–300                                    | 2               | 3.3125                       | 1.427726845         | 1.197568503       |
|  | 300–400                                    | 2               | 0.846154                     | 0.590483731         | 0.535140695       |
|  | 400–450                                    | 2               | 1.888889                     | 1.177549936         | 1.002417734       |
|  | 450–500                                    | 2               | 4.090909                     | 2.566043877         | 1.990085279       |
| 1:4/1.0  | 23–100                                     | 4               | 1.321429                     | 0.294169424         | 0.278817514       |
|  | 100–200                                    | 4               | 0.939394                     | 0.318407098         | 0.286080297       |
|  | 200–300                                    | 4               | 2.038462                     | 0.626056888         | 0.501480908       |
|  | 300–400                                    | 4               | 1.466667                     | 0.424283973         | 0.330548465       |
|  | 400–450                                    | 4               | 2.125                        | 0.621320931         | 0.458097595       |
|  | 450–500                                    | 4               | 3.214286                     | 1.324592548         | 0.87044946        |
| 1:10/1.0   | 23–100                                     | 10.71479        | 1.232143                     | 0.306299243         | 0.304717761       |
|  | 100–200                                    | 10.71479        | 0.674242                     | 0.247935587         | 0.255958151       |
|  | 200–300                                    | 10.71479        | 0.653846                     | 0.283080909         | 0.295824115       |
|  | 300–400                                    | 10.71479        | 1.806667                     | 0.414463152         | 0.432368357       |
|  | 400–450                                    | 10.71479        | 2                            | 0.435875842         | 0.460241775       |
|  | 450–500                                    | 10.71479        | 0.607143                     | 0.394999443         | 0.449018354       |
| 1:10/1:2   | 23–100                                     | 5.357394        | 1.642857                     | 0.669936379         | 0.673724249       |
|  | 100–200                                    | 5.357394        | 1.059524                     | 0.570706379         | 0.613067433       |
|  | 200–300                                    | 5.357394        | 1.0625                       | 0.645567871         | 0.706446919       |
|  | 300–400                                    | 5.357394        | 1.042308                     | 0.576815916         | 0.69998178        |
|  | 400–450                                    | 5.357394        | 1.777778                     | 0.826087685         | 1.00710967        |
|  | 450–500                                    | 5.357394        | 0.772727                     | 0.765205801         | 1.026578633       |
| 1:10/1:4   | 23–100                                     | 2.678697        | 0.932432                     | 1.041234127         | 1.092893185       |
|  | 100–200                                    | 2.678697        | 0.717742                     | 0.778675699         | 0.894707374       |
|  | 200–300                                    | 2.678697        | 0.320755                     | 0.452164834         | 0.589901052       |
|  | 300–400                                    | 2.678697        | 1.231818                     | 0.976853189         | 1.308033169       |
|  | 400–450                                    | 2.678697        | 0.941176                     | 0.701530916         | 1.004680619       |
|  | 450–500                                    | 2.678697        | 0.188889                     | 0.298204488         | 0.515846554       |

**Table 5.** Version I. The obtained values using computing.

| Model/Prototype<br>(All Protected with<br>Intumescent Paint) | Tmin-Tmax<br>$\Delta t$ [°C] | Values Considered to Be<br>Reference Ones |                           |                         | Values Obtained with the <i>ML</i> |                         |                  |
|--|------------------------------|---|---------------------------|-------------------------|------------------------------------|-------------------------|------------------|
|  |                              | $S_{A_{tr}}$ [–]                          | $S_{\dot{Q}_{total}}$ [–] | $S_{\dot{Q}_{eff}}$ [–] | $S_{\dot{Q}_{total}}$ [–]          | $S_{\dot{Q}_{eff}}$ [–] | $S_{A_{tr}}$ [–] |
| 1:2/1.0  | 23–100                       | 0.25                                      | 0.609609                  | 0.603051                | 0.609609                           | 0.603051                | 0.25             |
|  | 100–200                      | 0.25                                      | 0.682686                  | 0.656078                | 0.682686                           | 0.656078                | 0.25             |
|  | 200–300                      | 0.25                                      | 0.712561                  | 0.680468                | 0.712561                           | 0.680468                | 0.25             |
|  | 300–400                      | 0.25                                      | 0.41454                   | 0.356357                | 0.41454                            | 0.356357                | 0.25             |
|  | 400–450                      | 0.25                                      | 0.469012                  | 0.406216                | 0.469012                           | 0.406216                | 0.25             |
|  | 450–500                      | 0.25                                      | 0.656982                  | 0.556682                | 1.306933                           | 0.556682                | 0.25             |
| 1:4/1:2  | 23–100                       | 0.25                                      | 0.365176                  | 0.349882                | 0.365176                           | 0.349882                | 0.25             |
|  | 100–200                      | 0.25                                      | 0.496494                  | 0.464178                | 0.496494                           | 0.464178                | 0.25             |
|  | 200–300                      | 0.25                                      | 0.431012                  | 0.36153                 | 0.431012                           | 0.36153                 | 0.25             |
|  | 300–400                      | 0.25                                      | 0.697844                  | 0.632439                | 0.697844                           | 0.632439                | 0.25             |
|  | 400–450                      | 0.25                                      | 0.623409                  | 0.530692                | 0.623409                           | 0.530692                | 0.25             |
|  | 450–500                      | 0.25                                      | 0.627255                  | 0.486465                | 0.627255                           | 0.486465                | 0.25             |
| 1:4/1.0  | 23–100                       | 0.0625                                    | 0.222615                  | 0.210997                | 0.222615                           | 0.210997                | 0.0625           |
|  | 100–200                      | 0.0625                                    | 0.338949                  | 0.304537                | 0.338949                           | 0.304537                | 0.0625           |
|  | 200–300                      | 0.0625                                    | 0.307122                  | 0.24601                 | 0.307122                           | 0.24601                 | 0.0625           |
|  | 300–400                      | 0.0625                                    | 0.289285                  | 0.225374                | 0.289285                           | 0.225374                | 0.0625           |
|  | 400–450                      | 0.0625                                    | 0.292386                  | 0.215575                | 0.292386                           | 0.215575                | 0.0625           |
|  | 450–500                      | 0.0625                                    | 0.412095                  | 0.270806                | 0.412095                           | 0.270806                | 0.0625           |
| 1:10/1.0   | 23–100                       | 0.008                                     | 0.248591                  | 0.247307                | 0.248591                           | 0.247307                | 0.008            |
|  | 100–200                      | 0.008                                     | 0.367725                  | 0.379623                | 0.367725                           | 0.379623                | 0.008            |
|  | 200–300                      | 0.008                                     | 0.432947                  | 0.452437                | 0.432947                           | 0.452437                | 0.008            |
|  | 300–400                      | 0.008                                     | 0.229408                  | 0.239318                | 0.229408                           | 0.239318                | 0.008            |
|  | 400–450                      | 0.008                                     | 0.217938                  | 0.230121                | 0.217938                           | 0.230121                | 0.008            |
|  | 450–500                      | 0.008                                     | 0.650587                  | 0.73956                 | 0.650587                           | 0.73956                 | 0.008            |
| 1:10/1:2   | 23–100                       | 0.03199                                   | 0.407787                  | 0.410093                | 0.407787                           | 0.410093                | 0.0399           |
|  | 100–200                      | 0.03199                                   | 0.538644                  | 0.578625                | 0.538644                           | 0.578625                | 0.0319           |
|  | 200–300                      | 0.03199                                   | 0.607593                  | 0.664891                | 0.607593                           | 0.664891                | 0.0319           |
|  | 300–400                      | 0.03199                                   | 0.553403                  | 0.671569                | 0.553403                           | 0.671569                | 0.0319           |
|  | 400–450                      | 0.03199                                   | 0.464674                  | 0.566499                | 0.464674                           | 0.566499                | 0.0319           |
|  | 450–500                      | 0.03199                                   | 0.990266                  | 1.328514                | 0.990266                           | 1.328514                | 0.0319           |
| 1:10/1:4   | 23–100                       | 0.12799                                   | 1.116686                  | 1.172088                | 1.116686                           | 1.172088                | 0.1279           |
|  | 100–200                      | 0.12799                                   | 1.084896                  | 1.246559                | 1.084896                           | 1.246559                | 0.1279           |
|  | 200–300                      | 0.12799                                   | 1.40969                   | 1.839103                | 1.40969                            | 1.839103                | 0.1279           |
|  | 300–400                      | 0.12799                                   | 0.793017                  | 1.061872                | 0.793017                           | 1.061872                | 0.1279           |
|  | 400–450                      | 0.12799                                   | 0.745377                  | 1.067473                | 0.745377                           | 1.067473                | 0.1279           |
|  | 450–500                      | 0.12799                                   | 1.57873                   | 2.730952                | 1.57873                            | 2.730952                | 0.1279           |

**Table 6.** Version II. Values obtained using direct measurements.

| Model/Prototype<br>(All Protected with<br>Intumescent Paint) | Tmin-Tmax<br>Δt [°C] | Measured Values |                              |                           |                         |
|--|----------------------|-----------------|------------------------------|---------------------------|-------------------------|
|  |                      | $S_{\zeta}$ [–] | $S_{\Delta\tau_{total}}$ [–] | $S_{\dot{Q}_{total}}$ [–] | $S_{\dot{Q}_{eff}}$ [–] |
| 1:2/1.0  | 23–100               | 2               | 0.75                         | 0.609609                  | 0.603051                |
|  | 100–200              | 2               | 0.636364                     | 0.682686                  | 0.656078                |
|  | 200–300              | 2               | 0.615385                     | 0.712561                  | 0.680468                |
|  | 300–400              | 2               | 1.733333                     | 0.41454                   | 0.356357                |
|  | 400–450              | 2               | 1.125                        | 0.469012                  | 0.406216                |
|  | 450–500              | 2               | 0.785714                     | 0.656982                  | 0.556682                |
| 1:4/1:2  | 23–100               | 2               | 1.761905                     | 0.365176                  | 0.349882                |
|  | 100–200              | 2               | 1.47619                      | 0.496494                  | 0.464178                |
|  | 200–300              | 2               | 3.3125                       | 0.431012                  | 0.36153                 |
|  | 300–400              | 2               | 0.846154                     | 0.697844                  | 0.632439                |
|  | 400–450              | 2               | 1.888889                     | 0.623409                  | 0.530692                |
|  | 450–500              | 2               | 4.090909                     | 0.627255                  | 0.486465                |
| 1:4/1.0  | 23–100               | 4               | 1.321429                     | 0.222615                  | 0.210997                |
|  | 100–200              | 4               | 0.939394                     | 0.338949                  | 0.304537                |
|  | 200–300              | 4               | 2.038462                     | 0.307122                  | 0.24601                 |
|  | 300–400              | 4               | 1.466667                     | 0.289285                  | 0.225374                |
|  | 400–450              | 4               | 2.125                        | 0.292386                  | 0.215575                |
|  | 450–500              | 4               | 3.214286                     | 0.412095                  | 0.270806                |
| 1:10/1.0   | 23–100               | 10.71479        | 1.232143                     | 0.248591                  | 0.247307                |
|  | 100–200              | 10.71479        | 0.674242                     | 0.367725                  | 0.379623                |
|  | 200–300              | 10.71479        | 0.653846                     | 0.432947                  | 0.452437                |
|  | 300–400              | 10.71479        | 1.806667                     | 0.229408                  | 0.239318                |
|  | 400–450              | 10.71479        | 2                            | 0.217938                  | 0.230121                |
|  | 450–500              | 10.71479        | 0.607143                     | 0.650587                  | 0.73956                 |
| 1:10/1:2   | 23–100               | 5.357394        | 1.642857                     | 0.407787                  | 0.410093                |
|  | 100–200              | 5.357394        | 1.059524                     | 0.538644                  | 0.578625                |
|  | 200–300              | 5.357394        | 1.0625                       | 0.607593                  | 0.664891                |
|  | 300–400              | 5.357394        | 1.042308                     | 0.553403                  | 0.671569                |
|  | 400–450              | 5.357394        | 1.777778                     | 0.464674                  | 0.566499                |
|  | 450–500              | 5.357394        | 0.772727                     | 0.990266                  | 1.328514                |
| 1:10/1:4   | 23–100               | 2.678697        | 0.932432                     | 1.116686                  | 1.172088                |
|  | 100–200              | 2.678697        | 0.717742                     | 1.084896                  | 1.246559                |
|  | 200–300              | 2.678697        | 0.320755                     | 1.40969                   | 1.839103                |
|  | 300–400              | 2.678697        | 1.231818                     | 0.793017                  | 1.061872                |
|  | 400–450              | 2.678697        | 0.941176                     | 0.745377                  | 1.067473                |
|  | 450–500              | 2.678697        | 0.188889                     | 1.57873                   | 2.730952                |

**Table 7.** Version II. The obtained values using computing.

| Model/Prototype<br>(All Protected with<br>Intumescent Paint) | Values Considered to Be<br>Reference Ones |                     |                   | Values Obtained with the <i>ML</i> |                   |                  |
|--|---|---------------------|-------------------|------------------------------------|-------------------|------------------|
|  | $S_{A_{tr}}$ [–]                          | $S_{Q_{total}}$ [–] | $S_{Q_{eff}}$ [–] | $S_{Q_{total}}$ [–]                | $S_{Q_{eff}}$ [–] | $S_{A_{tr}}$ [–] |
|  | 0.25                                      | 0.457206            | 0.452289          | 0.457206                           | 0.452289          | 0.25             |
|  | 0.25                                      | 0.434437            | 0.417504          | 0.434437                           | 0.417504          | 0.25             |
| 1:2/1.0  | 0.25                                      | 0.438499            | 0.418749          | 0.438499                           | 0.418749          | 0.25             |
|  | 0.25                                      | 0.718536            | 0.617685          | 0.718536                           | 0.617685          | 0.25             |
|  | 0.25                                      | 0.527639            | 0.456993          | 0.527639                           | 0.456993          | 0.25             |
|  | 0.25                                      | 0.5162              | 0.437393          | 0.5162                             | 0.437393          | 0.25             |
|  | 0.25                                      | 0.643406            | 0.616459          | 0.643406                           | 0.616459          | 0.25             |
|  | 0.25                                      | 0.732919            | 0.685216          | 0.732919                           | 0.685216          | 0.25             |
|  | 0.25                                      | 1.427727            | 1.197569          | 1.427727                           | 1.197569          | 0.25             |
| 1:4/1:2  | 0.25                                      | 0.590484            | 0.535141          | 0.590484                           | 0.535141          | 0.25             |
|  | 0.25                                      | 1.17755             | 1.002418          | 1.17755                            | 1.002418          | 0.25             |
|  | 0.25                                      | 2.566044            | 1.990085          | 2.566044                           | 1.990085          | 0.25             |
|  | 0.0625                                    | 0.294169            | 0.278818          | 0.294169                           | 0.278818          | 0.0625           |
|  | 0.0625                                    | 0.318407            | 0.28608           | 0.318407                           | 0.28608           | 0.0625           |
| 1:4/1.0  | 0.0625                                    | 0.626057            | 0.501481          | 0.626057                           | 0.501481          | 0.0625           |
|  | 0.0625                                    | 0.424284            | 0.330548          | 0.424284                           | 0.330548          | 0.0625           |
|  | 0.0625                                    | 0.621321            | 0.458098          | 0.621321                           | 0.458098          | 0.0625           |
|  | 0.0625                                    | 1.324593            | 0.870449          | 1.324593                           | 0.870449          | 0.0625           |
|  | 0.008                                     | 0.306299            | 0.304718          | 0.306299                           | 0.304718          | 0.008            |
|  | 0.008                                     | 0.247936            | 0.255958          | 0.247936                           | 0.255958          | 0.008            |
| 1:10/1.0   | 0.008                                     | 0.283081            | 0.295824          | 0.283081                           | 0.295824          | 0.008            |
|  | 0.008                                     | 0.414463            | 0.432368          | 0.414463                           | 0.432368          | 0.008            |
|  | 0.008                                     | 0.435876            | 0.460242          | 0.435876                           | 0.460242          | 0.008            |
|  | 0.008                                     | 0.394999            | 0.449018          | 0.394999                           | 0.449018          | 0.008            |
|  | 0.031999                                  | 0.669936            | 0.673724          | 0.669936                           | 0.673724          | 0.031998         |
|  | 0.031999                                  | 0.570706            | 0.613067          | 0.570706                           | 0.613067          | 0.031999         |
| 1:10/1:2   | 0.031999                                  | 0.645568            | 0.706447          | 0.645568                           | 0.706447          | 0.031999         |
|  | 0.031999                                  | 0.576816            | 0.699982          | 0.576816                           | 0.699982          | 0.031999         |
|  | 0.031999                                  | 0.826088            | 1.00711           | 0.826088                           | 1.00711           | 0.031999         |
|  | 0.031999                                  | 0.765206            | 1.026579          | 0.765206                           | 1.026579          | 0.031999         |
|  | 0.127994                                  | 1.041234            | 1.092893          | 1.041234                           | 1.092893          | 0.127994         |
|  | 0.127994                                  | 0.778676            | 0.894707          | 0.778676                           | 0.894707          | 0.127994         |
| 1:10/1:4   | 0.127994                                  | 0.452165            | 0.589901          | 0.452165                           | 0.589901          | 0.127994         |
|  | 0.127994                                  | 0.976853            | 1.308033          | 0.976853                           | 1.308033          | 0.127994         |
|  | 0.127994                                  | 0.701531            | 1.004681          | 0.701531                           | 1.004681          | 0.127994         |
|  | 0.127994                                  | 0.298204            | 0.515847          | 0.298204                           | 0.515847          | 0.127994         |

One has to mention that for the amount of heat  $Q$ , the two cases presented before were considered, namely  $Q_{total}$  [J] and  $Q_{eff}$  [J], respectively, and correspondingly the heat flows were  $\dot{Q}_{total}$  [W] and  $\dot{Q}_{eff}$  [W], respectively.

The following values were obtained in a similar manner for Version II:

One can observe that the *ML* offers the same magnitudes for all involved variables and consequently these *MLs* will be very suitable for experimental simulations of complex structures, such as industrial halls with compartments, respective different kinds of floors, structures with one or multiple fire foci located on the structure, or as desired. One other significant aspect consists of the fact that the collected data measured on the models, i.e.,

their responses to the action of the fires, will serve by means of the obtained and validated *ML* to optimise real structures subjected to fires.

#### 4. Discussion and Conclusions

The influence of the existence of the intumescent layer on the heat exchange, as well as on the effective heating of the structural elements, represented a shield in front of the heat flow produced by the fire. This thermoprotective layer prevents the transfer of heat between the structural element and the surrounding environment, ensuring that it heats up more slowly and thus preserves its original load-bearing capacity for a longer time during the fire. The authors' previous investigations [62] were able to demonstrate an important thing regarding the influence of the actual heat exchange on the direction of the heat flow introduced into the system (i.e., the way of heating the structural element being tested). This is a curious thing at first glance, but it was true; it was also demonstrated that the size of the heat transfer coefficient will have practically the same value (showing differences only to the fourth decimal place!) regardless of the direction of the introduction of the heat flow into the system. Consequently, regardless of whether the pole is heated from the outside, as it is in the case of a real fire, or from the inside, as was the case with the help of this original electric stand by the authors [62], the size of the heat transfer coefficients, so finally the heat exchanges, will have identical values.

This fact, demonstrated on the basis of some precision measurements taken by the authors, allowed them to design an original electric stand [62,63], based on the heat flow directed in the opposite direction (from the inside to the outside), which was used in all subsequent investigations.

It should be emphasised that this method of heating, as well as the stand itself, bring significant improvements to the fire tests of the structural elements. Currently, special voluminous chambers heated with gas are used, meaning a rather difficult control of the evaluation and reproducibility of the thermal flow introduced into the system (therefore, in the tested structural element), but also much more rigorous conditions for the prevention of fires during their operation. The authors replaced this type of testing with much cheaper electrical stands, with a modern electronic control, which are safer in operation (without the danger of fires during the tests), and also ensure rigorous and reproducible control of the heating of the elements being tested [1,56,62,64–67].

Since we are talking about the use of heat flow in the opposite direction to that of fires, the structural element covered with the intumescent layer, under the same amount of heat introduced, will heat up faster and will reach higher temperatures. These effects can be observed if comparisons are made of the experimental data of thermally protected structural elements (covered with an intumescent layer) with those not thermally protected [1,56,62,64].

Based on the obtained results one can formulate the following:

1. The deduced *MLs* by the authors in the work [57], for two experimentally significant versions I and II, were validated by rigorous experimental investigations on multiple sets of prototypes and models;
2. One can see the facilities of MDA in evidence, for instance regarding the *ML* simplification, starting from the general case up to different particular ones [56–58,64];
3. It is also worth highlighting those simplifications related to ignoring several scale factors, involved in the following:
  - i. existing implicit correlations (having the same material for the prototype and the model; having identical environmental and deployment conditions for both of them);
  - ii. existing over-definition of the parameters (e.g., accepting the same scale of all lengths);
4. The variables of the different thicknesses ( $\delta_{y\ steel}$ ,  $\delta_{z\ steel}$ ) can help conceive various suitable models, e.g., with different wall thicknesses along ( $y$ ,  $z$ ) without any restriction on the geometric similarity of the prototype and model cross-sections;

5. The simultaneous inclusion of both length ( $L_z$ ) and shape factor ( $\zeta$ ) in the independent variables ensures a wide generalisation of the associated model to the analysed prototype; in this case, this meant no restrictions of geometric similarity and, additionally, one can accept models having other shapes of the cross-section, imposing only the same scale factor for ( $\zeta$ );
6. If ( $\lambda_{x \text{ steel}}$ ) is accepted as the independent variable, then another material can be chosen for the model with respect to the prototype and consequently both the manufacturing as well as the testing cost can be reduced;
7. By means of ( $Q$ ) or ( $\dot{Q}$ ) as an independent variable, one can choose a very convenient thermal stress strategy of the model with respect to the prototype;
8. If ( $\Delta t$ ) is selected as an independent variable, the thermal regime can be optimised from the point of view of loading the model in relation to the prototype. By means of the exposure time ( $\tau$ ) as an independent variable, one can obtain some supplementary benefits in order to more efficiently follow the thermal transfer to the analysed structure on fire;
9. In the authors' opinion, based on their multiple experiences in different fields of engineering, MDA can become a useful tool for common researchers in this field of thermal transfer phenomena and, last but not least, in the analysis of the complex phenomenon of fires in metal resistance structures. The obtained *ML* for straight bars can be extended to structural elements formed by straight bars, having the same cross-sections, which are obviously found in all civil and industrial structures. Consequently, these *MLs* will become useful tools in fire simulations as well as fire prevention research;
10. Taking into consideration the identity of the directly measured data with those obtained by *MLs* in Tables 5–8, it becomes possible to conceive high-accuracy, repetitive and very efficient thermal loading strategies for new, untested structural elements, which also represent a great/major advantage of MDA.

The authors' further goal consists of enlarging their use in buildings' fire protection optimisation.

**Author Contributions:** (P.-B.G., R.-I.S., I.S., S.V., T.G., K.J., Z.A. and G.P.): All the authors have equal contribution in conceptualisation; methodology; software; validation; formal analysis; investigation; resources; data curation; writing—original draft preparation; writing—review and editing; visualisation; supervision; project administration and funding acquisition. All authors have read and agreed to the published version of the manuscript.

**Funding:** This research received no external funding. The APC was funded by Transilvania University of Brasov.

**Institutional Review Board Statement:** Not applicable.

**Informed Consent Statement:** Not applicable.

**Data Availability Statement:** Not applicable.

**Conflicts of Interest:** The authors declare no conflict of interest.

## References

1. Munteanu (Száva), I.R. Investigation Concerning Temperature Field Propagation along Reduced Scale Modelled Metal Structures. Ph.D. Thesis, Transilvania University of Brasov, Braşov, Romania, 2018.
2. Aglan, A.A.; Redwood, R.G. Strain-Hardening Analysis of Beams with 2 WEB- Rectangular Holes. *Arab. J. Sci. Eng.* **1987**, *12*, 37–45.
3. Al-Homoud, M.S. Performance characteristics and practical applications of common building thermal insulation materials. *Build. Environ.* **2005**, *40*, 353–366. [[CrossRef](#)]
4. Bahrami, A.; Mousavi Anijdan, S.H.; Ekrami, A. Prediction of mechanical properties of DP steels using neural network model. *J. Alloy. Compd.* **2005**, *392*, 177–182. [[CrossRef](#)]
5. Bailey, C. Indicative fire tests to investigate the behaviour of cellular beams protected with intumescent coatings. *Fire Saf. J.* **2004**, *39*, 689–709. [[CrossRef](#)]

6. Dai, S.J.; Zhu, B.C.; Chen, Q. Analysis of bending strength of the rectangular hole honeycomb beam. In Proceedings of the 2nd International Conference on Civil, Architectural and Hydraulic Engineering, Progress in Industrial and Civil Engineering II, Zhuhai, China, 27–28 July 2013; PTS 1-4 405-408. pp. 993–999.
7. Deshwal, P.S.; Nandal, J.S. On Torsion of Rectangular Beams with Holes at the Center. *Indian J. Pure Appl. Math.* **1991**, *22*, 425–438.
8. John, A.; Bakowski, H.; Száva, I.; Vlase, S. New Tribological Aspects in the Micro-Areas of the Symmetric Rolling-Sliding Contact. *Symmetry* **2022**, *14*, 1523. [[CrossRef](#)]
9. Ferro, V. Assessing flow resistance law in vegetated channels by dimensional analysis and self-similarity. *Flow Meas. Instrum.* **2019**, *69*, 101610. [[CrossRef](#)]
10. Fourier, J. *Theorie Analytique de la Chaleur*; Firmin Didot: Paris, France, 1822. (In French)
11. Han, X.; Sun, X.; Li, G.; Huang, S.; Zhu, P.; Shi, C.; Zhang, T. A Repair Method for Damage in Aluminum Alloy Structures with the Cold Spray Process. *Materials* **2021**, *14*, 6957. [[CrossRef](#)]
12. Khan, M.A.; Shah, I.A.; Rizvi, Z.; Ahmad, J. A numerical study on the validation of thermal formulations towards the behaviours of RC beams. *Sci. Mater. Today Proc.* **2019**, *17*, 227–234. [[CrossRef](#)]
13. Lawson, R.M. Fire engineering design of steel and composite Buildings. *J. Constr. Steel Res.* **2001**, *57*, 1233–1247. [[CrossRef](#)]
14. Levac, M.L.J.; Soliman, H.M.; Ormiston, S.J. Three-dimensional analysis of fluid flow and heat transfer in single- and two-layered micro-channel heat sinks. *Heat Mass Transf.* **2011**, *47*, 1375–1383. [[CrossRef](#)]
15. Noack, J.; Rolfes, R.; Tessler, J. New layerwise theories and finite elements for efficient thermal analysis of hybrid structures. *Comput. Struct.* **2003**, *81*, 2525–2538. [[CrossRef](#)]
16. Papadopoulos, A.M. State of the art in thermal insulation materials and aims for future developments. *Energy Build.* **2005**, *37*, 77–86. [[CrossRef](#)]
17. Quintier, G.J. *Fundamentals of Fire Phenomena*; John Wiley & Sons: Hoboken, NJ, USA, 2006.
18. Şova, M.; Şova, D. *Thermotechnics, VL.II.*; Transilvania University Press: Transilvania, Romania, 2001.
19. Tafreshi, A.M.; di Marzo, M. Foams and gels as temperature protection agents. *Fire Saf. J.* **1999**, *33*, 295–305. [[CrossRef](#)]
20. Vlase, S.; Năstac, C.; Marin, M.; Mihalca, M. A Method for the Study of the Vibration of Mechanical Bars Systems with Symmetries. *Acta Tech. Napoc. Ser. Appl. Math. Mech. Eng.* **2017**, *60*, 539–544.
21. Wong, M.B.; Ghojel, J.I. Sensitivity analysis of heat transfer formulations for insulated structural steel components. *Fire Saf. J.* **2003**, *38*, 187–201. [[CrossRef](#)]
22. Yang, K.-C.; Chen, S.-J.; Lin, C.C.; Lee, H.H. Experimental study on local buckling of fire-resisting steel columns under fire load. *J. Constr. Steel Res.* **2005**, *61*, 553–565. [[CrossRef](#)]
23. Baker, W.; Baker, W.; Westine, P.S.; Dodge, F.T. *Similarity Methods in Engineering Dynamics*; Elsevier: Amsterdam, The Netherlands, 1991.
24. Carabogdan, G.I.; Badea, A.; Brătianu, C.; Muşatescu, V.I. *Methods of Analysis of Thermal Energy Processes and Systems*; Energy Processes and Systems: Ed. Tehn.: Bucharest, Romania, 1989.
25. Sedov, I.L. *Similarity and Dimensional Methods in Mechanics*; MIR Publisher: Moscow, Russia, 1982.
26. Yen, P.H.; Wang, J.C. Power generation and electrical charge density with temperature effect of alumina nanofluids using dimensional analysis. *Energy Convers. Manag.* **2009**, *186*, 546–555. [[CrossRef](#)]
27. Alshqirate, A.A.Z.S.; Tarawneh, M.; Hammad, M. Dimensional Analysis and Empirical Correlations for Heat Transfer and Pressure Drop in Condensation and Evaporation Processes of Flow Inside Micropipes: Case Study with Carbon Dioxide (CO<sub>2</sub>). *J. Braz. Soc. Mech. Sci. Eng.* **2012**, *34*, 89–96. [[CrossRef](#)]
28. Asgari, O.; Saidi, M. Three-dimensional analysis of fluid flow and heat transfer in the microchannel heat sink using additive-correction multigrad technique. In Proceedings of the Micro/Nanoscale Heat Transfer International Conference, PTS A AND B. 1st ASME Micro/Nanoscale Heat Transfer International Conference, Tainan, Tainan, Taiwan, 6–9 January 2008; pp. 679–689.
29. Barenblatt, G.I. *Dimensional Analysis*; Gordon and Breach: New York, NY, USA, 1987.
30. Barr, D.I.H. Consolidation of Basics of Dimensional Analysis. *J. Eng. Mech. ASCE* **1984**, *110*, 1357–1376. [[CrossRef](#)]
31. Bhaskar, R.; Nigam, A. Qualitative Physics using Dimensional Analysis. *Artif. Intell.* **1990**, *45*, 73–111. [[CrossRef](#)]
32. Bridgeman, P.W. *Dimensional Analysis*; Yale University Press: New Haven, CT, USA, 1922; (Reissued in paperbound in 1963).
33. Buckingham, E. On Physically Similar Systems. *Phys. Rev.* **1914**, *4*, 345. [[CrossRef](#)]
34. Canagaratna, S.G. Is dimensional analysis the best we have to offer. *J. Chem. Educ.* **1993**, *70*, 40–43. [[CrossRef](#)]
35. Carinena, J.F.; Santander, M. Dimensional Analysis. *Adv. Electron. Electron Phys.* **1988**, *72*, 181–258. [[CrossRef](#)]
36. Carlson, D.E. Some New Results in Dimensional Analysis. *Arch. Ration. Mech. Anal.* **1978**, *68*, 191–210. [[CrossRef](#)]
37. Chen, W.K. Algebraic Theory of Dimensional Analysis. *J. Frankl. Inst.* **1971**, *292*, 403–409. [[CrossRef](#)]
38. Coyle, R.G.; Ballicolay, B. Concepts and Software for Dimensional Analysis in Modeling. *IEEE Trans. Syst. Man Cybern.* **1984**, *14*, 478–487. [[CrossRef](#)]
39. Gibbings, J.C. Dimensional Analysis. *J. Phys. A-Math. Gen.* **1980**, *13*, 75–89. [[CrossRef](#)]
40. Gibbings, J.C. A Logic of Dimensional Analysis. *J. Physiscs A-Math. Gen.* **1982**, *15*, 1991–2002. [[CrossRef](#)]
41. Illan, F.; Viedma, A. Experimental study on pressure drop and heat transfer in pipelines for brine based ice slurry Part II: Dimensional analysis and rheological Model. *Int. J. Refrig. Rev. Int. Du Froid* **2009**, *32*, 1024–1031. [[CrossRef](#)]
42. Jofre, L.; del Rosario, Z.R.; Iaccarino, G. Data-driven dimensional analysis of heat transfer in irradiated particle-laden turbulent flow. *Int. J. Multiph. Flow* **2020**, *125*, 103198. [[CrossRef](#)]

43. Kivade, S.B.; Murthy, C.S.N.; Vardhan, H. The use of Dimensional Analysis and Optimisation of Pneumatic Drilling Operations and Operating Parameters. *J. Inst. Eng. India Ser. D* **2012**, *93*, 31–36. [[CrossRef](#)]
44. Langhaar, H.L. *Dimensional Analysis and Theory of Models*; John Wiley & Sons Ltd.: New York, NY, USA, 1951.
45. Martins, R.D.A. The Origin of Dimensional Analysis. *J. Frankl. Inst.* **1981**, *311*, 331–337. [[CrossRef](#)]
46. Nakla, M. On fluid-to-fluid modeling of film boiling heat transfer using dimensional analysis. *Int. J. Multiph. Flow* **2011**, *37*, 229–234. [[CrossRef](#)]
47. Nezhad, A.H.; Shamsoddini, R. Numerical Three-Dimensional Analysis of the Mechanism of Flow and Heat Transfer in a Vortex Tube. *Therm. Sci.* **2009**, *13*, 183–196. [[CrossRef](#)]
48. Pankhurst, R.C. *Dimensional Analysis and Scale Factor*; Chapman & Hall Ltd.: London, UK, 1964.
49. Remillard, W.J. Applying Dimensional Analysis. *Am. J. Phys.* **1983**, *51*, 137–140. [[CrossRef](#)]
50. Romberg, G. Contribution to Dimensional Analysis. *Ingenieur. Archiv.* **1985**, *55*, 401–412. [[CrossRef](#)]
51. Schnittger, J.R. Dimensional Analysis in Design. *Journal of Vibration, Acoustic. Stress Reliab. Des. Trans. ASME* **1988**, *110*, 401–407. [[CrossRef](#)]
52. Szekeres, P. Mathematical Foundations of Dimensional Analysis and the Question of Fundamental Units. *Int. J. Theor. Phys.* **1978**, *17*, 957–974. [[CrossRef](#)]
53. Yao, S.; Yan, K.; Lu, S.; Xu, P. Prediction and application of energy absorption characteristics of thinwalled circular tubes based on dimensional analysis. *Thin-Walled Struct.* **2018**, *130*, 505–519. [[CrossRef](#)]
54. Zierrep, J. *Similarity Laws and Modelling*; Marcel Dekker: New York, NY, USA, 1971.
55. Gálfi, B.-P.; Száva, I.; Şova, D.; Vlase, S. Thermal Scaling of Transient Heat Transfer in a Round Cladded Rod with Modern Dimensional Analysis. *Mathematics* **2021**, *9*, 1875. [[CrossRef](#)]
56. Száva, I.R.; Şova, D.; Dani, P.; Élesztős, P.; Száva, I.; Vlase, S. Experimental Validation of Model Heat Transfer in Rectangular Hole Beams Using Modern Dimensional Analysis. *Mathematics* **2022**, *10*, 409. [[CrossRef](#)]
57. Şova, D.; Száva, I.R.; Jármay, K.; Száva, I.; Vlase, S. Modern method to analyze the Heat Transfer in a Symmetric Metallic Beam with Hole. *Symmetry* **2022**, *14*, 769. [[CrossRef](#)]
58. Trif, I.; Asztalos, Z.; Kiss, I.; Élesztős, P.; Száva, I.; Popa, G. Implementation of the Modern Dimensional Analysis in Engineering Problems-Basic Theoretical Layouts. *Ann. Fac. Eng. Hunedoara* **2019**, *17*, 73–76, ISSN-L 1584-2665, Tome XVII, Fascicule 3 [August].
59. Szirtes, T. The Fine Art of Modelling, SPAR. *J. Eng. Technol.* **1992**, *1*, 37.
60. Szirtes, T. *Applied Dimensional Analysis and Modelling*; McGraw-Hill: Toronto, ON, Canada, 1998.
61. Száva, I.; Szirtes, T.; Dani, P. An Application of Dimensional Model Theory in the Determination of the Deformation of a Structure. *Eng. Mech.* **2006**, *13*, 31–39.
62. Dani, P.; Száva, I.R.; Kiss, I.; Száva, I.; Popa, G. Principle schema of an original full-, and reduced-scale testing bench, destined to fire protection investigations. *Ann. Fac. Eng. Hunedoara-Int. J. Eng.* **2018**, *16*, 149–152, Tome XVI, Fascicule 2.
63. Turzó, G.; Száva, I.R.; Gálfi, B.P.; Száva, I.; Vlase, S.; Hoța, H. Temperature distribution of the straight bar, fixed into a heated plane surface. *Fire Mater.* **2018**, *42*, 202–212. [[CrossRef](#)]
64. Száva, R.I.; Száva, I.; Vlase, S.; Gálfi, P.B.; Jármay, K.; Gălățanu, T.; Popa, G.; Asztalos, Z. Modern Dimensional Analysis-Based Steel Column Heat Transfer Evaluation using Multiple Experiments. *Symmetry* **2022**, *14*, 1952. [[CrossRef](#)]
65. Dani, P. Theoretical and Experimental Study of Heat-Field Propagation through Multi-Layer Fire-Protection on Stress-, and Strain-State of Metallic Structures. Ph.D. Thesis, Transilvania University of Brasov, Brasov, Romania, 2011.
66. Turzó, G. Temperature distribution along a straight bar sticking out from a heated plane surface and the heat flow transmitted by this bar (I)-Theoretical Approach. *Ann. Fac. Eng. Hunedoara-Int. J. Eng.* **2016**, *14*, 49–53, Tome XIV, Fascicule 3, ISSN:1584-2665.
67. Turzó, G.; Száva, I.R.; Dancsó, S.; Száva, I.; Vlase, S.; Munteanu, V.; Gălățanu, T.; Asztalos, Z. A New Approach in Heat Transfer Analysis: Reduced-Scale Straight Bars with Massive and Square-Tubular Cross-Sections. *Mathematics* **2022**, *10*, 3680. [[CrossRef](#)]